Polyhedron 28 (2009) 1029–1039

Contents lists available at ScienceDirect

Polyhedron

journal homepage: www.elsevier.com/locate/poly

Diphenyllead(IV) thiosemicarbazonates and pyrazolonates: Synthesis and characterization

José S. Casas [a,*], Eduardo E. Castellano [b], Javier Ellena [b], María S. García-Tasende [a], Agustín Sánchez [a,*], José Sordo [a], Ángeles Touceda [a]

[a] Departamento de Química Inorgánica, Facultade de Farmacia, Universidade de Santiago de Compostela, 15782 Santiago de Compostela, Galicia, Spain
[b] Instituto de Física de Sao Carlos, Universidade de Sao Paulo, Caixa Postal 369, CEP 13560 Sao Carlos, SP, Brazil

ARTICLE INFO

Article history:
Received 11 December 2008
Accepted 9 January 2009
Available online 13 February 2009

Dedicated to Professor Alfredo Mederos on the occasion of his retirement.

Keywords:
Diphenyllead(IV) complexes
Cyclization
Thiosemicarbazone ligands
Pyrazolone ligands
X-ray diffraction
^{1}H, ^{13}C and ^{207}Pb NMR

ABSTRACT

Cyclization of thiosemicarbazones derived from β-keto esters and β-keto amides (HTSC) in the presence of diphenyllead(IV) acetate was explored in methanol solution at room temperature and under reflux. All β-keto ester TSCs underwent cyclization to give the corresponding pyrazolone (HL), which, except in one case, deprotonated and coordinated the $PbPh_2^{2+}$ moiety to form homoleptic $[PbPh_2(L)_2]$ or heteroleptic $[PbPh_2(OAc)(L)]$ derivatives. Cyclization did not occur with β-keto amide TSCs and only $[PbPh_2(TSC)_2]$ or $[PbPh_2(OAc)(TSC)]$ thiosemicarbazonates were isolated. The complexes were characterized by IR spectroscopy in the solid state and by ^{1}H, ^{13}C and ^{207}Pb NMR spectroscopy in DMSO–d_6 solution, in which they evolve and decompose with time. Additionally, crystals of *p*-acetoacetanisidide thiosemicarbazone ($HTSC^{10}$), $[PbPh_2(OAc)(L^5)] \cdot MeOH$ (HL^5 = 2,5-dihydro-3,4-dimethyl-5-oxo-1*H*-pyrazolone-1-carbothioamide), $[PbPh_2Cl(L^2)]$ (HL^2 = 2,5-dihydro-5-oxo-3-phenyl-1*H*-pyrazolone-1-carbothioamide), $[PbPh_2(OAc)(TSC^8)] \cdot 2MeOH$ ($HTSC^8$ = acetoacetanilide thiosemicarbazone), $[PbPh_2(OAc)(TSC^{10})] \cdot H_2O$ and $[PbPh_2(OAc)(TSC^{11})] \cdot 0.75MeOH$ ($HTSC^{11}$ = *o*-acetoacetotoluidide) were studied by X-ray crystallography. The complexes, monomers or dimers with almost linear C–Pb–C moieties, are compared with the corresponding derivatives of Pb(II).

1. Introduction

Monothiosemicarbazones ($HTSC^n$) derived from 1,3-dicarbonyl compounds can undergo chain-to-ring evolution (Scheme 1) [1].

This interesting phenomenon is promoted by certain metal ions and leads to the formation of 5-pyrazolone (HL^n) derivatives, usually under mild conditions [2]. Several factors influence this reaction, but two of these are decisive for the viability of the process. The first factor is intrinsic and is related to the nature of the R_3 group, with the TSCs derived from β-keto esters being more prone to cyclization than those obtained from β-keto amides. The second factor, which is extrinsic, is the identity of the metal promoter. Thus, ions such as Zn(II) are less effective, with regard to the activation of the cycle formation, than Cd(II) [3].

The first factor can be rationalized by considering the proposed cyclization scheme [Ref. [3], see Scheme 2], in which the process starts with the complexation of the metal ion by the TSC after deprotonation. This step is followed by the nucleophilic attack of the deprotonated N(2) atom on the $C(O)R_3$ group and the loss of the R_3^- anion.

The RO^- groups are better leaving groups than the RNH^- groups and, as a result, step (II) → [III] is more easily accomplished when the TSCs are derived from β-keto esters. It has also been suggested that the formation of an N(4)–H···N(2) hydrogen bond is possible in the β-keto amide TSCs, and this intramolecular union can slow down the nucleophilic attack of N(2) on the carbonyl group [3].

At present, the origin of the influence of the metal ion is less clear and more experimental evidence is needed to rationalize this aspect of the reaction. As Zn(II) is a "borderline" acid and Cd(II) a "soft" acid according to the HSAB principle of Pearson [4], and taking into account that the two ions behave differently with respect to the cyclization – with the former less effective than the latter – it is possible that the influence of the metal may be related to its classification according to the HSAB principle.

In order to further explore this possibility, we recently reacted several $HTSC^n$ with Pb(II) ions [2]. In accordance with the "borderline" character of this ion [4], only a limited number of TSCs derived from β-keto amides (one of three) underwent cyclization. In the work described here, we analyzed the evolution of several $HTSC^n$ (see Scheme 3) caused by the $Ph_2Pb(IV)$ cation, for which the same "borderline" character has been proposed on the grounds of structural evidence [5]. As far as possible, in order to avoid the

* Corresponding authors. Tel.: +34 981 528074; fax: +34 981 547102 (A. Sánchez).
E-mail addresses: sergio.casas@usc.es (J.S. Casas), agustin.sanchez@usc.es (A. Sánchez).

0277-5387/$ - see front matter © 2009 Elsevier Ltd. All rights reserved.
doi:10.1016/j.poly.2009.01.004

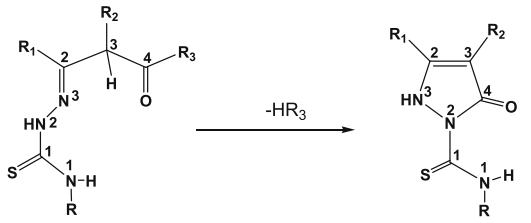

Scheme 1.

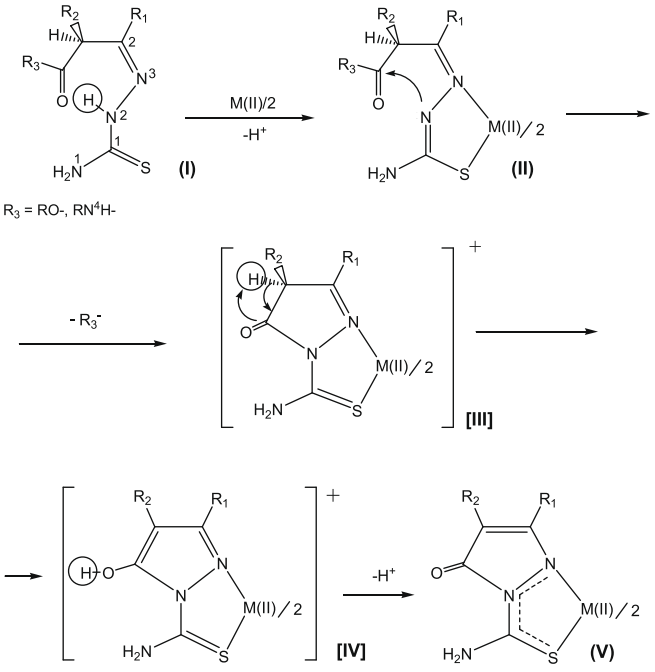

Scheme 2.

interference of other factors, we maintained the same experimental conditions used in the Pb(II) reactions: namely, the same solvent, identical counter-ion (AcO^-) and similar temperature. As described below, if there is a direct relationship between cyclization capacity and acid behaviour in terms of the HSAB principle, then Ph_2Pb(IV) seems to be "harder" than Pb(II).

2. Experimental

2.1. Physical measurements

Elemental analyses were performed on a Fisons instruments EA1108CHNS-O microanalyser. Melting points (m.p.), uncorrected, were determined with a Büchi apparatus. The electrospray mass spectra of the complexes were measured on a Hewlett–Packard model LC-MSD 1100 instrument (positive ion mode, 98:2 MeOH/HCOOH as mobile phase, 20–100 V). IR spectra were recorded from KBr discs on a Bruker IFS66V FT-IR spectrometer and are reported in cm^{-1}. The ^1H, ^{13}C and ^{207}Pb NMR spectra of DMSO-d_6 solutions were recorded on Bruker DPX 250, AMX 300 or AMX 500 instruments; chemical shifts are expressed on the δ scale (downfield shifts positive) relative to tetramethylsilane using the solvent signal for ^1H and ^{13}C NMR spectra and using a saturated solution of Ph_4Pb in $CDCl_3$ (−178 ppm) as the external reference for ^{207}Pb spectra. All spectroscopic measurements were carried out at the RIAIDT services of the University of Santiago de Compostela.

2.2. Materials

Thiosemicarbazide (Merck), N^1-ethylthiosemicarbazide (Merck), methyl acetoacetate (Aldrich), ethyl benzoylacetate (Aldrich), methyl 4-methoxyacetoacetate (Aldrich), methyl propionoylacetate (Aldrich), ethyl 2-methylacetoacetate (Aldrich), ethyl 2-ethylacetoacetate (Aldrich), acetoacetanilide (Merck), *o*-acetoacetanisidide (Aldrich), *p*-acetoacetanisidide (Aldrich), *o*-acetoacetotoluidide (Aldrich), silver acetate (Probus), and diphenyl- lead(IV) chloride (ABCR) were used as received. Diphenyllead(IV) acetate was prepared *in situ* by stirring diphenyllead(IV) chloride and silver acetate in methanol for 5 h. The resulting AgCl precipitate was filtered off and the solution containing the organolead(IV) acetate was used immediately in the preparation of the complexes.

2.3. Synthesis of ligands

The thiosemicarbazone ligands derived from β-dicarbonyl compounds (β-keto esters and β-keto amides) were prepared according to the method described by Jayasree and Aravindakshan [6]. Physical and analytical properties of $HTSC^n$ (n = 1–10) and HL^n (n = 1–7) have been reported elsewhere [3,7]. Recrystallization of $HTSC^{10}$ from EtOH gave crystals suitable for X-ray analysis.

The synthesis and physical and spectroscopic properties of $HTSC^{11}$ are described below.

$HTSC^{11}$. A mixture of *0*-acetoacetotoluidide (1.90 g, 10 mmol) and thiosemicarbazide (0.90 g, 10 mmol) in ethanol (125 ml) was heated under reflux for 1 h. The resulting white solid was filtered off and dried under vacuum. M.p.: 158 °C. *Anal.* Calc. for $C_{12}H_{16}N_4OS$: C, 54.5; H, 6.1; N, 21.2; S, 12.1. Found: C, 54.6; H, 6.0; N, 20.8; S, 11.9%. IR (cm^{-1}): 3443 s, 3280 s, 3163 m, ν(N–H); 1651 s, ν(C=O); 1600 s, ν(C=N); 1497 s, 1247 w, ν(NH–Ph); 1023 m, 850 w, ν(C=S). ^1H NMR: 10.43 s, 10.15 s, 9.67 s, 9.44 s [(2), $N_{(2/4)}H$]; 8.14 s, 7.67 s, 7.63 s [(2), $N_{(1)}H_2$]; 7.36–7.08 m [(4), $H_{8\text{-}11}$]; 3.56 s, 3.40 s [(2), $C_{(3)}H_2$]; 2.20 s, 2.17 s [(3), $C_{(12)}H_3$]; 2.03 s, 1.99 s [(3), $C_{(5)}H_3$]. ^{13}C NMR: 178.8 [$C_{(1)}$]; 167.1 [$C_{(4)}$]; 149.0 [$C_{(2)}$]; 136.0–125.1 [$C_{(6-11)}$]; 46.0 [$C_{(3)}$]; 17.8 [$C_{(12)}$]; 16.7 [$C_{(5)}$].

2.4. Synthesis of complexes

General procedure [*Caution! Organolead(IV) compounds are very toxic*] [8]. A solution of freshly prepared $PbPh_2(OAc)_2$ in methanol was mixed in 1:2 or 1:1 molar ratio with a solution or suspension of the thiosemicarbazone ligand in the same solvent. The resulting mixtures were stirred for 6 h at room temperature or under reflux. The experimental conditions and the complexes obtained are summarized in Table 1. Only the reaction between $PbPh_2(OAc)_2$ and $HTSC^4$ gave unidentified products under all conditions. Details for each reaction are described in Supplementary data.

The analytical, physical and spectroscopic data for the complexes obtained are listed below.

$[PbPh_2Cl(L^2)]$. Colour: yellow. M.p.: 191 °C (d). *Anal.* Calc. for $C_{22}H_{18}N_3OSClPb$: C, 42.96; H, 2.95; N, 6.83; S, 5.21. Found: C, 42.79; H, 3.10; N, 6.82; S, 5.09%. IR (cm^{-1}): 3283 s, 3111 w, 3058 s, ν(N–H); 1612 s, ν(C=O); 1578 s, ν(ring); 1402 s, ν(C–N); 922 m, 764 m, ν(C=S). ^1H NMR: 11.80 bs, 9.93 bs [(2) $N_{(1)}H_2$]; 8.03 d (4) [H_oPh_2Pb]; 7.63 t (4) [H_mPh_2Pb]; 7.47 t (2) [H_pPh_2Pb]; 7.38 m (2) [$C_{(6,10)}H$]; 7.28 m (3) [$C_{(7-9)}H$]; 5.87 s, 5.45 br s [(1) $C_{(3)}H$].

$[PbPh_2(L^2)_2]$. Colour: yellow. M.p.: 163 °C (d). *Anal.* Calc. for $C_{30}H_{28}N_6O_2S_2Pb$: C, 46.44; H, 3.64; N, 10.83; S, 8.26. Found: C, 47.45; H, 3.31; N, 10.74; S, 8.78%. MS (electrospray), m/z (%): 161 (100) [(H_2B)+H−{$NH_2C(S)$}]. IR (cm^{-1}): 3295 s, 3160 w, 3118 s,

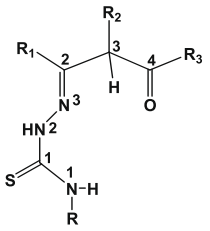

I (HTSC^n)

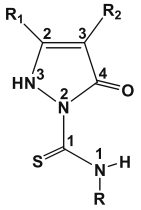

II(HL^n)

I/II	R	R_1	R_2	R_3
HTSC^1/HL^1	-H	$-\overset{5}{C}H_3$	-H	$-O\overset{6}{C}H_3$
HTSC^2/HL^2	-H		-H	$-O\overset{11}{C}H_2\overset{12}{C}H_3$
HTSC^3/HL^3	-H	$-\overset{5}{C}H_2O\overset{6}{C}H_3$	-H	$-O\overset{7}{C}H_3$
HTSC^4/HL^4	-H	$-CH_2CH_3$	-H	$-OCH_3$
HTSC^5/HL^5	-H	$-\overset{5}{C}H_3$	$-\overset{6}{C}H_3$	$-O\overset{7}{C}H_2\overset{8}{C}H_3$
HTSC^6/HL^6	-H	$-\overset{5}{C}H_3$	$-\overset{6}{C}H_2\overset{7}{C}H_3$	$-O\overset{8}{C}H_2\overset{9}{C}H_3$
HTSC^7/HL^7	$-\overset{5}{C}H_2\overset{6}{C}H_3$	$-\overset{7}{C}H_3$	-H	$-O\overset{8}{C}H_3$
HTSC^8/HL^1	-H	$-\overset{5}{C}H_3$	-H	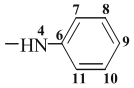
HTSC^9/HL^1	-H	$-\overset{5}{C}H_3$	-H	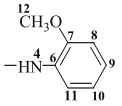
HTSC^{10}/HL^1	-H	$-\overset{5}{C}H_3$	-H	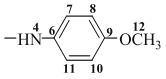
HTSC^{11}/HL^1	-H	$-\overset{5}{C}H_3$	-H	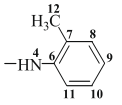

Scheme 3. Ligands used in this work or obtained by cyclization (see Scheme 1).

3064 w, *ν*(N–H); 1652 s, *ν*(C=O); 1369 s, *ν*(C–N); 1590 sh, *ν*(ring); 918 w, 765 m, *ν*(C=S). ^{1}H NMR: 12.19 br s, 9.96 br s [(4) $N_{(1)}H_2$]; 7.96 d [H_oPh_2Pb], $^3J(^1H–^{207}Pb)$ = 206.5 Hz; 7.85 s (4) [$C_{(6,10)}H$]; 7.67 t [H_mPh_2Pb]; 7.63 [H_oPh_2Pb]; 7.50 t [H_pPh_2Pb]; 7.45 s (6) [$C_{(7-9)}H$]; 7.37 t [H_mPh_2Pb]; 7.27 t [H_pPh_2Pb]; 6.06 bs, 5.87 s [(2) $C_{(3)}H$]. ^{13}C NMR: 175.8 [$C_{(1)}$]; 165.9 [$C_{(4)}$]; 160.9 [$C_{ipso}(Ph_2Pb)$]; 143.3 [$C_{(2)}$]; 135.8 [$C_o(Ph_2Pb)$], $^2J(^{13}C–^{207}Pb)$ = 90.0 Hz; 132.9 [$C_o(Ph_2Pb)$], $^2J(^{13}C–^{207}Pb)$ = 132.9 Hz; 130.3 [$C_m(Ph_2Pb)$]; 130.2 [$C_p(Ph_2Pb)$]; 130.0–124.5 [$C_{(5-10)}$]; 86.7 [$C_{(3)}$].

[PbPh$_2$(OAc)(L^2)]. Colour: yellow. M.p.: 135 °C (d). *Anal.* Calc. for $C_{24}H_{21}N_3O_3SPb$: C, 45.13; H, 3.31; N, 6.58; S, 5.02. Found: C, 44.62; H, 3.45; N, 6.18; S, 4.82%. MS (electrospray), *m*/*z* (%): 580 (25) [M–(OAc)]; 485 (47) [M–(2Ph)] ≡ [Pb(OAc)(L^2)]; 288 (63) [Pb(L^2)]–{(Ph)+(C(S)NH$_2$)}; 242 (22) HL^2+Na; 185 (23) (HL^2)+H+Na–{C(S)NH$_2$}; 161 (100) (HL^2)+H–{NH$_2$C(S)}. IR (cm^{-1}): 3138 w, 3053 m, *ν*(N–H); 1609 s, *ν*(C=O); 1567 s, 1398 s, *ν*(CH$_3$COO), (Δ*ν*: 169); 1385 s, *ν*(C–N); 1575 h, *ν*(ring); 921 m, 754 m, *ν*(C=S). ^{1}H NMR: 12.00–9.00 (2) [$N_{(1)}H_2$]; 8.30–7.00 m (15) [R_1(Ph)+H(Ph_2Pb)]; 5.87 s, 5,19 s [(1), $C_{(3)}H$]; 1.80 s (3) [CH_3COO]. ^{13}C NMR: 175.5 [$C_{(1)}$]; 166.5 [$C_{(4)}$]; 161.0 [$C_{ipso}(Ph_2Pb)$]; 143.3 [$C_{(2)}$]; 136.1 [$C_o(Ph_2Pb)$], $^2J(^{13}C–^{207}Pb)$ = 87.2 Hz; 132.9 [$C_o(Ph_2Pb)$], $^2J(^{13}C–^{207}Pb)$ = 128.0 Hz; 130.2 [$C_m(Ph_2Pb)$]; 130.0 [$C_p(Ph_2Pb)$]; 130.0–124.7 [$C_{(5-10)}$]; 86.8, 83.7 [$C_{(3)}$]; 23.2 [CH_3COO].

[PbPh$_2$Cl(TSC^3)]. Colour: white. M.p.: 135 °C. *Anal.* Calc. for $C_{19}H_{22}N_3O_3SClPb$: C, 37.10; H, 3.60; N, 6.83; S, 5.21. Found: C, 37.41; H, 3.60; N, 7.03; S, 5.27%. IR (cm^{-1}): 3478 s, 3358 s, 3170 w, 3053 w, *ν*(N–H); 1725 s, *ν*(C=O); 1597 s, *ν*(C=N); 1432 s, 1453 w, *δ*(OCH$_2$); 1247 w, *ν*(C–O); 1014 m, 744 s, *ν*(C=S). ^{1}H NMR: 7.92 d (4) [$H_o(Ph_2Pb)$], $^3J(^1H–^{207}Pb)$ = 110 Hz; 7.55 t (4) [$H_m(Ph_2Pb)$]; 6.93 s (2) [$N_{(1)}H_2$]; 3.97 s (2) [$C_{(5)}H_2$]; 3.61 s, 3.51 s [(2) $C_{(3)}H_2$]; 3.60 s (3) [$C_{(7)}H_3$]; 2.91 s (3) [$C_{(6)}H_3$]. ^{13}C NMR: 168.4 [$C_{(4)}$]; 159.8 [$C_{(2)}$]; 136.7 [$C_o(Ph_2Pb)$], $^2J(^{13}C–^{207}Pb)$ = 88 Hz; 129.9 [$C_m(Ph_2Pb)$]; 129.2 [$C_p(Ph_2Pb)$]; 74.7 [$C_{(5)}$]; 58.8 [$C_{(6)}$]; 52,1 [$C_{(7)}$]; 32.8 [$C_{(3)}$].

[Pb(L^3)$_2$]. See Ref. [2].

[PbPh$_2$(L^3)$_2$]. Colour: beige. M.p.: 121 °C. *Anal.* Calc. or $C_{24}H_{26}N_6O_4S_2Pb$: C, 39.28; H, 3.57; N, 11.45; S, 8.72. Found: C, 37.55; H, 3.73; N, 11.56; S, 9.05%. MS (electrospray), *m*/*z* (%): 548

Table 1
Reactions of $PbPh_2(OAc)_2$ with $HTSC^n$ in MeOH: conditions used and compounds obtained.

Ligand	M:L (mol ratio)	*T*	Compounds
$HTSC^1$	1:2	r.t.	HL[1a]
	1:1	r.t.	HL[1a]
$HTSC^2$	1:2	r.t.	unidentified product
		under reflux	$[PbPh_2(L^2)_2]$
	1:1	r.t.	$[PbPh_2Cl(L^2)]$
		under reflux	$[PbPh_2(OAc)(L^2)]$
$HTSC^3$	1:2	r.t.	$[PbPh_2Cl(TSC^3)]$
		under reflux	first fraction, $[Pb(L^3)_2]$
			second fraction, $[PbPh_2(L^3)_2]$
	1:1	r.t.	$[PbPh_2Cl(TSC^3)]$[b]
$HTSC^4$	1:1 and 1:2	r.t.	unidentified products
		under reflux	
$HTSC^5$	1:2	r.t.	first fraction, $[Pb(L^5)_2]$
			second fraction, $[PbPh_2(L^5)_2]\cdot H_2O$
		under reflux	$[Pb(OAc)(L^5)]$
	1:1	r.t.	unidentified product
		under reflux	first fraction, $[Pb(OAc)(L^5)]$
			second fraction, $[PbPh_2(OAc)(L^5)]\cdot MeOH$
$HTSC^6$	1:2	r.t.	$[PbPh_2(L^6)_2]$[c]
	1:1	r.t.	$[PbPh_2(OAc)(L^6)]$
$HTSC^7$	1:2 or 1:1	r.t.	$[PbPh_2(OAc)(L^7)]$[c]
$HTSC^8$	1:2 or 1:1	r.t.	$[PbPh_2(OAc)(TSC^8)]\cdot 2MeOH$[c]
$HTSC^9$	1:2	r.t.	$[PbPh_2(TSC^9)_2]$
	1:1	r.t.	first fraction, $[PbPh_2(TSC^9)_2]$[d]
			second fraction, $[PbPh_2(OAc)(TSC^9)]$[e]
$HTSC^{10}$	1:2 or 1:1	r.t.	$[PbPh_2(OAc)(TSC^{10})]\cdot H_2O$[c]
$HTSC^{11}$	1:2 or 1:1	r.t.	$[PbPh_2(OAc)(TSC^{11})]\cdot 0.75MeOH$[c]

[a] The same compound was obtained when the reaction mixture was heated under reflux for 6 h.
[b] The reaction of this ligand under reflux afforded unidentified products when a 1:1 molar ratio was used.
[c] The same compound was obtained when 1:2 or 1:1 molar ratios were heated under reflux for 6 h.
[d] The same compound was obtained when 1:2 or 1:1 (second fraction) molar ratios were heated under reflux for 6 h.
[e] The same compound was obtained when a 1:1 (first fraction) molar ratio was heated under reflux for 6 h.

(98) [M–(L^3)]. IR (cm^{-1}): 3277 s, 3094 w, 3055 w, *ν*(N–H); 1663 m, *ν*(C=O); 1369 s, *ν*(C–N); 1580 s, 1517 m, *ν*(ring); 903 m, 760 w, *ν*(C=S). ^{1}H NMR: 11.59 s, 9.64 s [(4) $N_{(1)}H_2$]; 7.98 d (4) [H_oPh_2Pb], $^3J(^1H–^{207}Pb)$ = 208 Hz; 7.57 t (4) [H_mPh_2Pb]; 7.42 t (2) [H_pPh_2Pb]; 4.60 s (2) [$C_{(3)}H$]; 4.37 s (4) [$C_{(5)}H_2$]; 3.30 s (6) [$C_{(6)}H_3$]. ^{13}C NMR: 175.7 [$C_{(1)}$]; 167.3 [$C_{(4)}$]; 157.6 [$C_{(2)}$]; 132.7 [$C_o(Ph_2Pb)$]; 130.2 [$C_m(Ph_2Pb)$]; 129.6 [$C_p(Ph_2Pb)$]; 81.9 [$C_{(3)}$]; 68.2 [$C_{(5)}$]; 58.5 [$C_{(6)}$]. ^{207}Pb NMR: −738.1.

[Pb(L^5)$_2$]. Colour: yellow. M.p.: 154 °C (d). *Anal*. Calc. for $C_{12}H_{16}N_6O_2S_2Pb$: C, 26.32; H, 2.94; N, 15.35; S, 11.71. Found: C, 26.14; H, 2.64; N, 15.24; S, 11.50%. ^{1}H NMR: 11.82 s, 9.65 s [(4) $N_{(1)}H_2$]; 2.08 s (6) [$C_{(5)}H_3$]; 1.61 s (6) [$C_{(6)}H_3$]. ^{13}C NMR: 175.2 [$C_{(1)}$]; 166.0 [$C_{(4)}$]; 90.7 [$C_{(3)}$]; 13.3 [$C_{(5)}$]; 6.4 [$C_{(6)}$].

[PbPh$_2$(L^5)$_2$] · H$_2$O. Colour: yellow. M.p.: 175 °C. *Anal*. Calc. or $C_{24}H_{28}N_6O_3S_2Pb$: C, 40.05; H, 3.92; N, 11.67; S, 8.91. Found: C, 40.63; H, 3.80; N, 10.9; S, 8.49%. IR (cm^{-1}): 3411 m, 3071 w, *ν*(N–H); 1645 s, *ν*(C=O); 1367 s, *ν*(C–N); 1576 m, 1518 m, *ν*(ring); 992 m, 762 w, *ν*(C=S). ^{1}H NMR: 11.75 s, 9.76 s [(4) $N_{(1)}H_2$]; 7.81 (4) [H_oPh_2Pb], $^3J(^1H–^{207}Pb)$ = 210 Hz; 7.56 (4) [H_mPh_2Pb]; 7.43 (2) [H_pPh_2Pb]; 2.07 s, 2.00 s [(6) $C_{(5)}H_3$]; 1.63 s (6) [$C_{(6)}H_3$].

[Pb(OAc)(L^5)]. See Ref. [2].

[PbPh$_2$(OAc)(L^5)]. Colour: yellow. M.p.: 138 °C (d). *Anal*. Calc. for $C_{20}H_{21}N_3O_3SPb$: C, 40.67; H, 3.58; N, 7.11; S, 5.43. Found: C, 40.36; H, 3.95; N, 6.52; S, 5.38%. MS (electrospray), *m*/*z* (%): 532 (18) [M+H–(C(S)NH_2)]; 485 (93) [M+H–{Ph+2CH_3}]; 407 (100) [M–{2Ph+2CH_3}] ≡ [Pb(OAc)(L^5–2CH_3)]. IR (cm^{-1}): 3295 m, 3053 m, *ν*(N–H); 1631 s, *ν*(C=O); 1559 m, 1401 m, *ν*(CH_3COO), (Δ*ν*: 158); 1368 m, *ν*(C–N); 1586 h, 1518 m, *ν*(ring); 909 w, 750 h, *ν*(C=S). ^{1}H NMR: 11.72 bs, 9.74 br s [(2) $N_{(1)}H_2$]; 7.84 d (4) [H_oPh_2Pb], $^3J(^1H–^{207}Pb)$ = 204 Hz; 7.55 t (4) [H_mPh_2Pb]; 7.41 m (2) [H_pPh_2Pb]; 2.03 s (3) [$C_{(5)}H_3$]; 1.82 s (3) [CH_3COO]; 1.62 s (3) [$C_{(6)}H_3$]. ^{13}C NMR: 175.2, 174.3, [$C_{(1)}$]; 167.7 [$C_{ipso}(Ph_2Pb)$]; 166.5, 165.6 [$C_{(4)}$]; 159.7, 158.2 [$C_{(2)}$]; 136.1–128.3 [C_o–$C_p(Ph_2Pb)$]; 95.5, 91.8 [$C_{(3)}$]; 23.1, 21,0 [CH_3COO]; 13.1, 9.8 [$C_{(5)}$]; 6.5, 6.3 [$C_{(6)}$]. ^{207}Pb NMR: −575.3, −871.9.

[PbPh$_2$(L^6)$_2$]. Colour: yellow. M.p.: 184 °C (d). *Anal*. Calc. for $C_{26}H_{30}N_6O_2S_2Pb$: C, 42.79; H, 4.14; N, 11.51; S, 8.78. Found: C, 42.41; H, 4.17; N, 11.28; S, 8.72%. MS (electrospray), *m*/*z* (%): 485 (100) [M–{L^6+C(S)NH_2}]; 407 (87) [PbMe(L^6)]. IR (cm^{-1}): 3414 w, *ν*(N–H); 1616 s, *ν*(C=O); 1369 s, *ν*(C–N); 1586 h, 1518 m, *ν*(ring); 967 m, 748 m, *ν*(C=S). ^{1}H NMR: 11.83 br s, 9.63 s [(4), $N_{(1)}H_2$]; 7.87 d (4) [H_oPh_2Pb]; 7.55 t (4) [H_mPh_2Pb]; 7.43 m (2) [H_pPh_2Pb]; 2.11 m (4) [$C_{(6)}H_2$]; 2.08 s (6) [$C_{(5)}H_3$]; 0.94 t (6) [$C_{(7)}H_3$]. ^{13}C NMR: 155.2 [$C_{(2)}$]; 136.9–128.1 [C_o–$C_p(Ph_2Pb)$]; 104.6 [$C_{(3)}$]; 15.0 [$C_{(6)}$]; 14.7 [$C_{(7)}$]; 13.4 [$C_{(5)}$]. ^{207}Pb NMR: −706.4.

[PbPh$_2$(OAc)(L^6)]. Colour: yellow. M.p.: 132 °C. *Anal*. Calc. for $C_{21}H_{23}N_3O_3SPb$: C, 41.71; H, 3.83; N, 6.93; S, 5.30. Found: C, 41.03; H, 3.62; N, 6.34; S, 5.13%. IR (cm^{-1}): 3138 m, 3055 m, *ν*(N–H); 1611 s, *ν*(C=O); 1564 s, 1405 m, *ν*(CH_3COO), (Δ*ν*: 159); 1370 h, *ν*(C–N); 1585 h, 1521 s, *ν*(ring); 938 w, 773 w, *ν*(C=S). ^{1}H NMR: 11.64 s, 9.71 s [(2), $N_{(1)}H_2$]; 7.81 d (4) [H_oPh_2Pb]; 7.60 m (4) [H_mPh_2Pb]; 7.46 m (2) [H_pPh_2Pb]; 2.11 m (2) [$C_{(6)}H_2$]; 2.02 s (3) [$C_{(5)}H_3$]; 1.81 s (3) [CH_3COO]; 0.95 t, 0.97 t [(3) $C_{(7)}H_3$]. ^{207}Pb NMR: −869.5.

[PbPh$_2$(OAc)(L^7)]. Colour: yellow. M.p.: 146 °C. *Anal*. Calc. for $C_{21}H_{23}N_3O_3SPb$: C, 41.71; H, 3.83; N, 6.93; S, 5.30. Found: C, 41.66; H, 3.74; N, 6.95; S, 5.38%. MS (electrospray), *m*/*z* (%): 578 (35) [M+H–(CH_2CH_3)]; 546 (100) [M–(OAc)]; 407 (18) [M–{2Ph+(NHCH_2CH_3)}] ≡ [Pb(OAc)(L^7–NHCH_2CH_3)]. IR (cm^{-1}): 3437 m, 3052 w, *ν*(N–H); 1609 s, *ν*(C=O); 1568 s, 1415 m, *ν*(CH_3COO), (Δ*ν*: 153); 1345m, *ν*(C–N); 1580 h, *ν*(ring); 947 m, 776 s, *ν*(C=S). ^{1}H NMR: 12.71 br s (2) [$N_{(1)}H_2$]; 7.81 d (4) [H_oPh_2Pb], $^3J(^1H–^{207}Pb)$ = 208 Hz; 7.56 m (4) [H_mPh_2Pb]; 7.41 m (2) [H_pPh_2Pb]; 4.70 s (1) [$C_{(3)}H$]; 3.50 br s (2) [$C_{(5)}H_2$]; 2.06 s (3) [$C_{(7)}H_3$]; 1.84 s (3) [CH_3COO]; 1.11 (3) [$C_{(6)}H_3$]. ^{13}C NMR: 179.6 [CH_3COO]; 174.4 [$C_{(1)}$]; 167.5 [$C_{(4)}$]; 167.1 [$C_{ipso}(Ph_2Pb)$]; 158.7

[$C_{(2)}$]; 132.2 [$C_o(Ph_2Pb)$]; 130.1 [$C_m(Ph_2Pb)$]; 129.7 [$C_p(Ph_2Pb)$]; 86.7 [$C_{(3)}$]; 23.4 [CH_3COO]; overlapped with the signal of DMSO-d_6 [$C_{(5)}$]; 14.6 [$C_{(6)}$]; 13.7 [$C_{(7)}$].

[$PbPh_2(OAc)(TSC^8)$] · 2MeOH. Colour: yellow. M.p.: 126 °C. *Anal.* Calc. for $C_{27}H_{34}N_4O_5SPb$: C, 44.19; H, 4.67; N, 7.63; S, 4.37. Found: C, 44.03; H, 4.62; N, 7.63; S, 4.00%. MS (electrospray), *m/z* (%): 611 (100) [M−(OAc)]; 407 (30) [$PbPh_2(HCOO)$]. IR (cm^{-1}): 3424 m, 3358 m, 3277 m, 3172 w, 3132 w, 3057 m, *ν*(N–H); 1651 s, *ν*(C=O); 1597 s, *ν*(C=N); 1566 sh, 1330 s, *ν*(CH_3COO), (Δ*ν*: 226); 1552 s, 1246 w, *ν*(NH–Ph); 1082 w, 872 w, *ν*(C=S). ^{1}H NMR: 10.25, 10.15, 10.04 [(1), $N_{(4)}H$]; 7.82 d (4) [H_oPh_2Pb], $^3J(^1H–^{207}Pb)$ = 111.4 Hz; 7.55 (2) [$C_{(7,11)}H$]; 7.52 t (4) [H_mPh_2Pb]; 7.35 m (2) [H_pPh_2Pb]; 7.29 (2) [$C_{(8,10)}H$]; 7.04 (1) [$C_{(9)}H$]; 7.00 s (2) [$N_{(1)}H_2$]; 4.09 m (2) [CH_3OH]; 3.16 d (6) [CH_3OH]; 1.98 s (3) [$C_{(5)}H_3$]; 1.74 s (3) [CH_3COO]. ^{13}C NMR: 167.3 [$C_{(4)}$]; 160.9 [$C_{ipso}(Ph_2Pb)$]; 155.3 [$C_{(2)}$]; 138.9–119.2 [C_{7-11}]; 136.3 [$C_o(Ph_2Pb)$], $^2J(^{13}C–^{207}Pb)$ = 88.5 Hz; 129.6 [$C_m(Ph_2Pb)$], $^3J(^{13}C–^{207}Pb)$ = 111.4 Hz; 128.8 [$C_p(Ph_2Pb)$]; 46.5 [$C_{(3)}$]; 23.7 [CH_3COO]; 18.5, 16.9 [$C_{(3)}$]. ^{207}Pb NMR: −294.5, −863.3.

[$PbPh_2(TSC^9)_2$]. Colour: white. M.p.: 181 °C (d). *Anal.* Calc. for $C_{36}H_{40}N_8O_4S_2Pb$: C, 47.00; H, 4.38; N, 12.18; S, 6.97. Found: C, 46.86; H, 4.40; N, 12.12; S, 7.08%. MS (electrospray), *m/z* (%): 943 (13) [M+Na]; 867 (4) [M+H+Na−(Ph)]; 641 (100) [M−(TSC^9)]. IR (cm^{-1}): 3439 w, 3408 w, 3338 m, 3301 m, 3189 m, 3051 m, *ν*(N–H); 1675 s, *ν*(C=O); 1602 s, *ν*(C=N); 1542 s, 1254 s, *ν*(NH–Ph); 1434m, *δ*(OCH_3); 1046 m, 897 w, *ν*(C=S). ^{1}H NMR: 10.08 br s, 9.80 br s, 9.52 br s, 9.28 s [(2) $N_{(4)}H$]; 8.00–7.00 m (10) [$H(Ph_2Pb)$]; 7.80–6.80 m (8) [$C_{(8-11)}H$]; 3.81 s (6) [$C_{(12)}H_3$]; 2.15 s, 1.98 s, 1.94 s [(6) $C_{(5)}H_3$]. ^{207}Pb NMR: −294.5.

[$PbPh_2(OAc)(TSC^9)$]. Colour: white. M.p.: 162 °C (d). *Anal.* Calc. for $C_{26}H_{28}N_4O_4SPb$: C, 44.63; H, 4.03; N, 8.01; S, 4.58. Found: C, 44.44; H, 4.26; N, 7.83; S, 4.41%. MS (electrospray) *m/z* (%): 641 (100) [M−(OAc)]; 518 (42) [M−{(OAc)+Ph+OCH_3+CH_3}]; 285 (55) [PbPh]. IR (cm^{-1}): 3437 w, 3404 m, 3380 m, 3300 m, 3189 m, *ν*(N–H); 1674 s, *ν*(C=O); 1602 s, *ν*(C=N); 1581 s, 1330, *ν*(CH_3COO), (Δ*ν*: 251); 1544 s, 1257 s, *ν*(NH–Ph); 1433 m, *δ*(OCH_3); 1024 m, 897 w, *ν*(C=S). ^{1}H NMR: 9.55 br s, 9.29 br s [(1) $N_{(4)}H$]; 7.88 m (1) [$C_{(11)}H$]; 7.80 d (4) [$H_o(Ph_2Pb)$], $^3J(^1H–^{207}Pb)$ = 112 Hz; 7.51 t (4) [$H_m(Ph_2Pb)$]; 7.35 t (2) [$H_p(Ph_2Pb)$]; 7.03 m (2) [$C_{(8,9)}H$]; 6.88 m (1) [$C_{(10)}H$]; 3.81 s (3) [$C_{(12)}H_3$]; 3.83 s, 3.73 s, 3.63 s, 3.38 s [(2) $C_{(3)}H_2$]; 2.00 s, 1.96 s [(3) $C_{(5)}H_3$]; 1.74 s (3) [CH_3COO]. ^{13}C NMR: 166.9 [$C_{(4)}$]; 160.6 [$C_{ipso}(Ph_2Pb)$]; 154.4 [$C_{(2)}$]; 149–110 [C_{7-11}]; 136.1 [$C_o(Ph_2Pb)$], $^2J(^{13}C–^{207}Pb)$ = 86.5 Hz; 129.3 [$C_m(Ph_2Pb)$], $^3J(^{13}C–^{207}Pb)$ = 111.2 Hz; 128.6 [$C_p(Ph_2Pb)$]; 55.6 [$C(_{12})H_3$]; 46.2 [$C_{(3)}$]; 16.9 [$C_{(5)}$]. ^{207}Pb NMR: −294.5.

[$PbPh_2(OAc)(TSC^{10})$] · H_2O. Colour: yellow. M.p.: 148 °C. *Anal.* Calc. for $C_{26}H_{30}N_4O_5SPb$: C, 43.51; H, 4.21; N, 7.81; S, 4.47. Found: C, 43.99; H, 4.44; N, 7.69; S, 4.45%. MS (electrospray). *m/z* (%): 641 (100) [M−(OAc)]; 485 (32) [$PbPh_3(HCOO)$+H]. IR (cm^{-1}): 3410 m, 3351 m, 3284 m, 3052 m, *ν*(N–H); 1646 s, *ν*(C=O); 1604 s, *ν*(C=N); 1580 s, 1331 m, *ν*(CH_3COO), (Δ*ν*: 249); 1552 s, 1237 s, *ν*(NH–Ph); 1434 m, *δ*(OCH_3); 1032 m, 836 m, *ν*(C=S). ^{1}H NMR: 10.20 s, 9.90 s [(1) $N_{(4)}H$]; 7.82 d (4) [$H_o(Ph_2Pb)$], $^3J(^1H–^{207}Pb)$ = 112.8 Hz; 7.52 t (4) [$H_m(Ph_2Pb)$], $^4J(^1H–^{207}Pb)$ = 58.4 Hz; 7.40 m (2) [$C_{(7,11)}H$]; 7.37 m (2) [$H_p(Ph_2Pb)$]; 6.86 d (2) [$C_{(8,10)}H$]; 3.70 s (3) [$C_{(12)}H_3$]; 1.98 s, 1.96 s [(3) $C_{(5)}H_3$]; 1.73 s (3) [CH_3COO]. ^{13}C NMR: 178.2 [$C_{(1)}$]; 166.7 [$C_{(4)}$]; 155.3–113.8 [$C_{(7-11)}$]; 136.2 [$C_o(Ph_2Pb)$]; 129.7 [$C_m(Ph_2Pb)$]; 129.0 [$C_p(Ph_2Pb)$]; 55.2 [$C_{(12)}$]; 46.3 [$C_{(3)}$]. ^{207}Pb NMR: −294.3.

[$PbPh_2(OAc)(TSC^{11})$] · 0.75MeOH. Colour: yellow. M.p.: 132 °C. *Anal.* Calc. for $C_{26.75}H_{31}N_4O_{3.75}SPb$: C, 45.39; H, 4.41; N, 7.92; S, 4.53. Found: C, 44.83; H, 4.65; N, 7.53; S, 4.17%. MS (electrospray). *m/z* (%): 625 (100) [M−(OAc)]. IR (cm^{-1}): 3432 m, 3368 w, 3267 m, 3157 m, 3053 m, *ν*(N–H); 1642 s, *ν*(C=O); 1602 h, *ν*(C=N); 1577 s, 1329 s, *ν*(CH_3COO), (Δ*ν*: 248); 1535 s, 1248 w, *ν*(NH–Ph); 1016 m, 850 w, *ν*(C=S). ^{1}H NMR: 10.15 br s, 9.64 br s, 9.42 s [(1) $N_{(4)}H$]; 7.82 d (4) [$H_o(Ph_2Pb)$], $^3J(^1H–^{207}Pb)$ = 113.2 Hz; 7.53 t (4) [$H_m(Ph_2Pb)$], $^4J(^1H–^{207}Pb)$ = 58.4 Hz; 7.37 m (2) [$H_p(Ph_2Pb)$]; 7.35–7.05 m (4) [$C_{(8-11)}H$]; 4.10 q (0.75) [CH_3OH]; 3.16 d (2.25) [CH_3OH]; 2.19 s, 2.17 s [(3) $C_{(12)}H_3$]; 2.03 s, 1.98 s [(3) $C_{(5)}H_3$]; 1.74 s (3) [CH_3COO]. ^{13}C NMR: 176.3 [$C_{(1)}$]; 167.2 [$C_{(4)}$]; 160.9 [$C_{ipso}(Ph_2Pb)$]; 157.7 [$C_{(2)}$]; 136.4–125.2 [$C_{(7-11)}$]; 136.3 [$C_o(Ph_2Pb)$], $^2J(^{13}C–^{207}Pb)$ = 87.2 Hz; 129.6 [$C_m(Ph_2Pb)$]; 128.9 [$C_p(Ph_2Pb)$]; 48.6 [$C_{(3)}$]; 17.8 [$C_{(12)}$]; 16.9 [$C_{(5)}$]. ^{207}Pb NMR: −191.9, −670.9, −862.8.

The following crystals, which were suitable for X-ray diffractometry, were obtained from the mother liquors of the specified reactions: [$PbPh_2Cl(L^2)$] ($PbPh_2(OAc)_2$/$HTSC^2$ reaction, 1:1 molar ratio, room temperature), [$PbPh_2(OAc)(L^5)$] · MeOH ($PbPh_2(OAc)_2$/TSC^5 reaction, 1:1 molar ratio, under reflux), [$PbPh_2(OAc)$-(TSC^8)] · 2MeOH ($PbPh_2(OAc)_2$/$HTSC^8$ reaction, 1:1 molar ratio, room temperature), [$PbPh_2(OAc)(TSC^{10})$] · H_2O ($PbPh_2(OAc)_2$/$HTSC^{10}$ reaction, 1:1 molar ratio, room temperature) and [$PbPh_2$-$(OAc)(TSC^{11})$] · 0.75MeOH ($PbPh_2(OAc)_2$/$HTSC^{11}$ reaction, 1:2 molar ratio, room temperature).

2.5. X-ray crystallography

Crystal data for $HTSC^{10}$, [$PbPh_2(OAc)(TSC^{10})$] · H_2O, [$PbPh_2$-$(OAc)(TSC^{11})$] · 0.75MeOH, [$PbPh_2Cl(L^2)$] and [$PbPh_2(OAc)(L^5)$] · MeOH were collected on a Nonius Kappa CCD (São Carlos Institute of Physics, University of São Paulo), and data for [$PbPh_2$-$(OAc)(TSC^8)$] · 2MeOH were obtained on a Bruker SMART CCD-1000 (RIAIDT, University of Santiago de Compostela). Structures were solved using direct methods for the ligand and the Patterson method for the complexes, followed by normal difference Fourier techniques and refined using SHELXS-97 [9]. Data were corrected for absorption by multi-scan [10] or SADABS [11]. All hydrogen atoms were introduced in calculated positions. Molecular graphics were obtained with ORTEP-3 [12], PLATON [13] and MERCURY [14]. Experimental details and crystal and refinement data are listed in Table 2.

3. Results and discussion

3.1. Syntheses and physical properties of the complexes

Diphenyllead(IV) reacts with TSCs derived from β-keto esters through cyclization processes similar to those induced by Pb(II). Differences in the complexes obtained (Table 1) can be related to the apparently slightly higher tendency of $PbPh_2^{2+}$ to form heteroleptic [$PbPh_2(OAc)(L)$] compounds instead of the homoleptic [$PbPh_2(L)_2$] type, suggesting a somewhat lower affinity of $PbPh_2^{2+}$ for the pyrazolonate anion than the Pb(II) cation. This lower affinity is particularly evident in the reaction with $HTSC^1$, which leads to free pyrazolone (HL^1) with the organometallic cation under all of the conditions tested, whereas with Pb(II) the [$Pb(L^1)_2$] complex is formed. However, the dephenylation reactions in which the organometallic cation take part, which transform $PbPh_2^{2+}$ into Pb(II), paradoxically contribute most to the differences between the products obtained when these TSCs are cyclized in the presence of $PbPh_2^{2+}$ and Pb(II) cations. Although these dephenylation processes can give rise to lead(II) pyrazolonates, very often these reactions are incomplete and lead to mixed compounds that are very difficult to separate and identify. Similar but fully evolved processes have previously been observed for the $PbPh_3^+$ and $PbMe_2^{2+}$ cations in the presence of ferrocenyl TSCs [15] and these results were related to the weakness of the Pb–C bonds [16]. It is worth noting that, in some cases, a minimal amount of the heteroleptic complexes containing Cl^- ligands were also isolated, probably because the $PbPh_2(OAc)_2$ used in the reaction was contaminated with some $PbPh_2Cl_2$ used in the synthesis of the former species (see Section 2).

Table 2
Crystallographic data for ligand and complexes.

	HTSC^{10}	[$PbPh_2(OAc)(TSC^8)$] · 2MeOH	[$PbPh_2(OAc)(TSC^{10})$] · H_2O	[$PbPh_2(OAc)(TSC^{11})$] · 0.75MeOH	[$PbPh_2(OAc)(L^5)$] · MeOH	[$PbPh_2Cl(L^2)$]
Empirical formula	$C_{12}H_{16}N_4O_2S$	$C_{27}H_{34}N_4O_5PbS$	$C_{26}H_{30}N_4O_5PbS$	$C_{26.75}H_{31}N_4O_{3.75}PbS$	$C_{21}H_{25}N_3O_4SPb$	$C_{22}H_{18}ClN_3OPbS$
Molecular weight	280.35	733.83	717.79	707.81	622.69	615.09
T (K)	140(2)	293(2)	140(2)	120(2)	120(2)	120(2)
λ (Å)	0.71073	0.71073	0.71073	0.71073	0.71073	0.71073
Crystal system	triclinic	orthorhombic	monoclinic	orthorhombic	triclínico	monoclínico
Space group	$P\bar{1}$	$Pna2_1$	$P2_1/n$	$Pna2_1$	$P\bar{1}$	$P2_1/n$
a (Å)	4.864(6)	19.539(4)	10.0550(2)	19.4506(4)	7.68970(10)	9.6303(8)
b (Å)	8.815(7)	9.7859(18)	18.7710(6)	10.0005(2)	11.7006(2)	14.3190(10)
c (Å)	16.657(15)	14.957(3)	15.0200(4)	14.9527(2)	12.7776(3)	97.727(4)
α (°)	102.12(5)	90	90	90	96.8530(10)	90
β (°)	90.76(7)	90	95.7340(10)	90	105.8530(10)	15.9170(10)
γ (°)	102.87(13)	90	90	90	90.4740(10)	90
V (Å^3)	679.40(12)	2859.9(9)	2820.73(13)	2908.54(9)	1097.02(3)	2175.0(3)
Z	2	4	4	4	2	4
D_{calc} (Mg/m^3)	1.370	1.704	1.690	1.616	1.885	1.878
μ (mm^{-1})	0.242	6.015	6.096	5.908	7.817	7.994
F(000)	296	1448	1408	1390	604	1176
Crystal size (mm)	0.60 × 0.40 × 0.12	0.27 × 0.13 × 0.11	0.06 × 0.04 × 0.02	0.18 × 0.17 × 0.12	0.30 × 0.11 × 0.05	0.11 × 0.08 × 0.07
θ range(°)	1.25–24.99	2.33–28.28	1.74–25.00	2.29–24.99	3.20–27.53	3.43–25.00
h; k; l range	−3, 5; −10, 10; −19, 19	0, 26; 0, 12; −9, 19	−11, 11; −22, 22; −17, 17	−23, 22; −11, 11; −17, 17	−9, 9; −15, 15; 0, 16	−11, 11; −15, 17; −18, 18
Max. and Min. transmission	0.9715–0.8682	0.407–0.516	0.715–0.544	0.5374–0.4161	0.6772–0.3730	0.6046–0.4734
Measured reflections	3086	16806	16655	23250	10112	9774
Unique reflections	2124	4985	4964	5021	5020	3816
R_{int}	0.0749	0.0392	0.0659	0.0748	0.0683	0.0958
R_1 ($I > 2\sigma I$)	0.1069	0.0258	0.0808	0.0438	0.0299	0.0512
wR_2 ($I > 2\sigma I$)	0.2681	0.0492	0.1941	0.1142	0.0677	0.1148
Goodness-of-fit	1.038	1.054	1.204	1.077	1.072	1.021
Deposit no.	712077	712078	712079	712080	712081	712082

Regarding the reactions of diphenyllead(IV) acetate with TSCs derived from β-keto amides, cyclization did not occur in any case and only thiosemicarbazonates were isolated. Note that Pb(II) forms the corresponding pyrazolonate with HTSC[8], although not with HTSC[9] or HTSC[10] [2]. Thus, if there is a relationship between cyclization and "soft" character, then $PbPh_2^{2+}$, although a "borderline" ion, might be a little "harder" than Pb(II).

The complexes are all solids and are mostly yellow in colour. The complexes are insoluble in water, soluble in DMSO and DMF but only sparingly soluble in ethanol and acetone.

3.2. X-ray studies

3.2.1. HTSC[10]

The atomic numbering scheme for this TSC ligand is shown in Fig. 1 and selected bonds lengths and angles are listed in Table 3. The structure shows some disorder that affects the atoms of the ring [C(7), C(8), C(10) and C(11)], which are delocalized between two equally populated positions.

The thiosemicarbazone chain adopts the E configuration around the C(2)–N(3) and C(1)–N(2) bonds with the sulfur atom trans to the N–N bond. The bonds lengths and angles are similar to those previously found for this type of compound [17]. The atoms of the molecule are distributed in two planes, SN(1)C(1)N(2)-N(3)C(2)C(5)C(3) [rms = 0.0668] and C(4)N(4)C(6)C(7)C(8)C(9)-C(10)C(11) [rms = 0.0976] which form a dihedral angle of 76.94(0.42)°.

There is an intermolecular hydrogen bond [N(1)–H(1A)···N(3)] that limits the free rotation of the $-N(1)H_2$ group around the N(1)–C(1) bond (see below) and there is also a weak intermolecular N(1)–H(1B)···S^i interaction that associates the molecules into pairs. Another intramolecular hydrogen bond [N(4)–H(4)···$O(1)^{ii}$] connects the pairs to give parallel chains along the *a* axis (Table 4, Fig. 1S).

3.2.2. Complexes

The molecular structures of the complexes $[PbPh_2(OAc)(TSC^8)] \cdot 2MeOH$, $[PbPh_2(OAc)(TSC^{10})] \cdot H_2O$ and $[PbPh_2(OAc)(TSC^{11})] \cdot 0.75MeOH$ are shown in Figs. 2–4 together with the numbering schemes. Selected bonds lengths and angles are listed in Table 5. The three structures include solvent molecules (MeOH or H_2O) in the lattice. In $[PbPh_2(OAc)(TSC^{10})] \cdot H_2O$, the water molecule is disordered over two positions with occupancies of 0.75:0.25. Only the molecule in the high-occupancy position has been included in Table 4. This disorder is probably responsible for the low quality of the collected data.

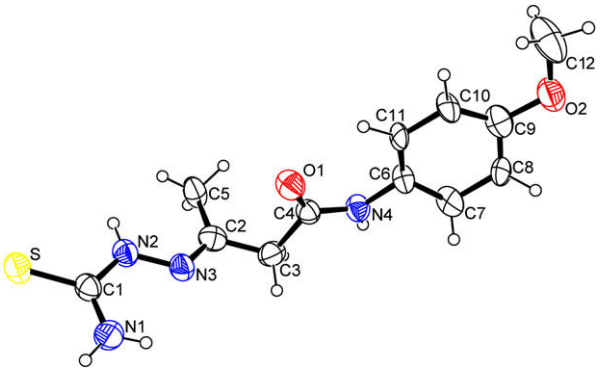

Fig. 1. Molecular structure of HTSC[10].

Table 3
Bond distances (Å) and angles (°) for HTSC[10].

S–C(1)	1.693(9)	C(1)–N(2)–N(3)	118.6(7)
O(1)–C(4)	1.239(10)	C(2)–N(3)–N(2)	117.5(7)
N(1)–C(1)	1.323(10)	N(1)–C(1)–N(2)	117.3(8)
N(2)–N(3)	1.403(10)	N(1)–C(1)–S(1)	124.2(7)
N(2)–C(1)	1.360(11)	N(2)–C(1)–S(1)	118.6(7)
N(3)–C(2)	1.295(11)	N(3)–C(2)–C(3)	115.0(7)
C(2)–C(3)	1.509(12)	C(2)–C(3)–C(4)	111.3(7)
C(3)–C(4)	1.545(11)	O(1)–C(4)–C(3)	120.7(8)

Table 4
Hydrogen bonds (Å, °) in ligand and complexes.

D–H···A	d(D–H)	d(H···A)	d(D···A)	<(DHA)
HL[10a]				
N(1)–H(1A)···N(3)	0.88	2.27	2.638(11)	105.1
N(1)–H(1B)···S^i	0.88	2.66	3.537(8)	175.9
N(4)–H(4)···$O(1)^{ii}$	0.88	2.02	2.884(10)	168.7
$[PbPh_2(OAc)(TSC^8)] \cdot 2MeOH$[b]				
N(1)–H(1B)···$O(4)^i$	0.86	2.34	3.188(8)	166.7
N(4)–H(4)···$O(2)^{ii}$	0.86	2.01	2.843(6)	163.9
O(4)–H(4A)···O(3)	0.82	1.86	2.679(6)	172.1
O(5)–H(5)···$O(4)^{iii}$	0.82	2.03	2.841(9)	170.8
$[PbPh_2(OAc)(TSC^{10})] \cdot H_2O$[c]				
N(1)–H(1B)···$O(1W)^i$	0.88	2.00	2.88(2)	173.6
N(4)–H(4)···$O(4)^i$	0.88	1.95	2.827(19)	174.1
O(1W)–H(12W)···$O(3)^{ii}$	0.80	2.13	2.755(19)	136.1
$[PbPh_2(OAc)(TSC^{11})] \cdot 0.75MeOH$[d]				
N(1)–H(1A)···N(3)	0.88	2.34	2.645(13)	100.7
N(1)–H(1B)···$O(1S)^i$	0.88	2.07	2.903(14)	156.8
O(1S)–H(1S)···O(2)	0.84	1.92	2.712(13)	157.8
N(4)–H(4)···$O(3)^{ii}$	0.88	1.95	2.782(11)	156.1
$[PbPh_2Cl(L^2)]$[e]				
N(1)–H(1A)···O	0.88	1.94	2.650(11)	136.4
N(1)–H(1B)···Cl^{ii}	0.88	2.50	3.355(9)	165.4
$[PbPh_2(OAc)(L^5)] \cdot MeOH$[f]				
N(1)–H(1A)···O(1)	0.88	1.93	2.633(4)	135.6
N(1)–H(1B)···$O(1S)^{ii}$	0.88	1.92	2.783(5)	166.9
O(1S)–H(1S)···O(1)	0.84	1.95	2.718(4)	151.1

[a] i: $-x+1, -y+1, -z$; ii: $x+1, y, z$.
[b] i: $-x+1/2, y-1/2, z+1/2$; ii: $-x+1/2, y-1/2, z-1/2$; iii: $x-1/2, -y+3/2, z$.
[c] i: $x-1/2, -y+1/2, z-1/2$; ii: $x, y, z+1$.
[d] i: $-x-1/2, y+1/2, z-1/2$; ii: $-x-1/2, y+1/2, z+1/2$.
[e] ii: $-x+3/2, y+1/2, -z+1/2$.
[f] ii: $-x, -y, -z+1$.

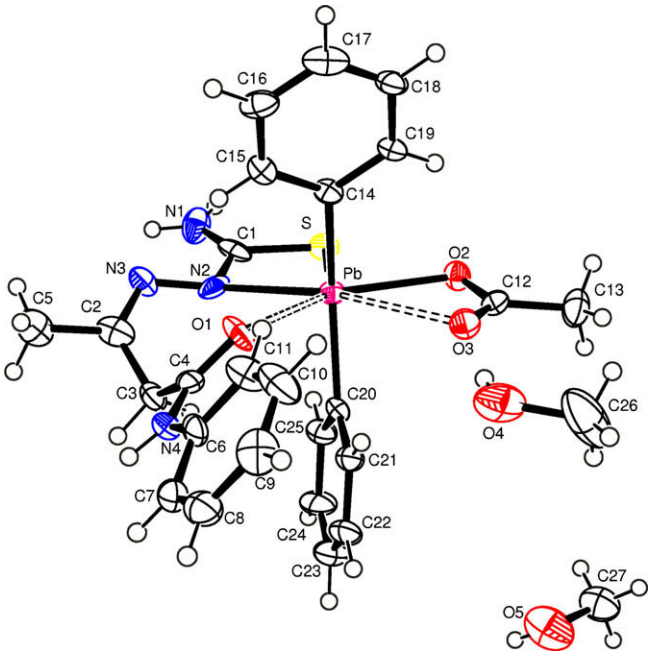

Fig. 2. Molecular structure of $[PbPh_2(OAc)(TSC^8)] \cdot 2MeOH$.

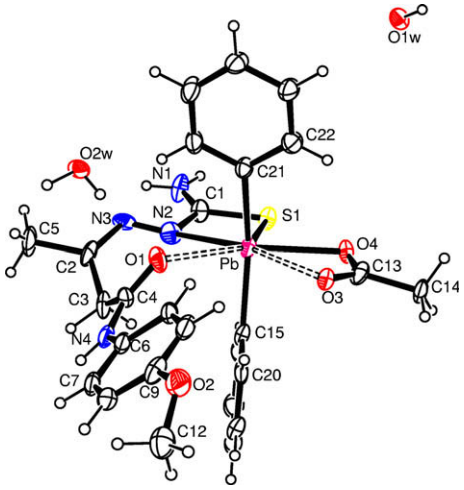

Fig. 3. Molecular structure of $[PbPh_2(OAc)(TSC^{10})] \cdot H_2O$.

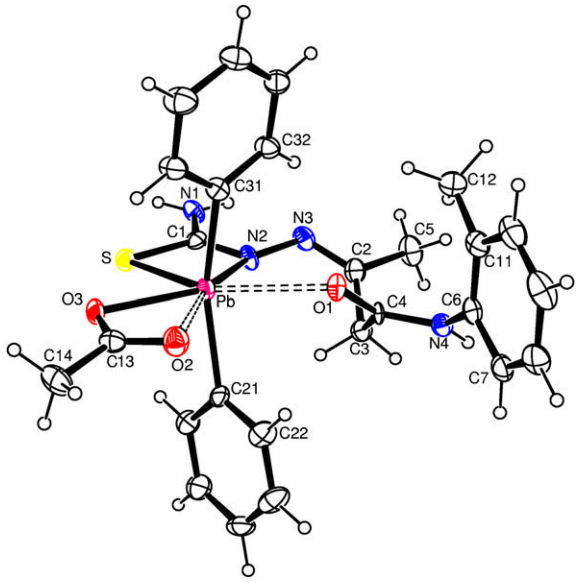

Fig. 4. Molecular structure of $[PbPh_2(OAc)(TSC^{11})] \cdot 0.75MeOH$ (methanol have been omitted for clarity).

As can be seen from the figures, in all three heteroleptic complexes the diphenyllead(IV) cation is bound to a TSC^- ligand and to an anisobidentate acetate. The thiosemicarbazonate interacts via its S, N(2) and O(1) donor atoms, with the last interaction probably being a weak one. Similarly, one of the lead–acetate bonds [Pb–O(3)] seems to be even weaker than Pb–O(1) judging by the bond distance (cf. 2.83–2.77 Å). If these weak Pb–O bonds are taken into account, then lead has a pentagonal bipyramidal coordination, with the donor atoms of both TSC^- and AcO^- ligands equatorial and the carbon atom of the phenyl groups apical.

The deprotonation and coordination of the thiosemicarbazonate to the metal give rise to some changes with respect to the structure of the free $HTSC^8$ and $HTSC^{10}$ ligands [7a]. In both cases the bonding to the metal increases the carbon–sulfur bond distances, suggesting a thione to thiol evolution of the thioamide group. Also, in order to achieve the coordination of O(4) along with that of S and N(2), the ligands must change its conformation about the C(2)═N(3) bond in the free state from E to Z.

The most conspicuous characteristic of these structures is the N(2),S-coordination mode adopted by the TSC^- anion in place of the more usual N(3),S-coordination (see, e.g. Ref. [7b]). This leads to a four-membered chelate ring (see Figs. 2–4) instead of the five-membered ring that is formed when the thiosemicarbazonate binds in the usual N(3),S-mode. The N(2),S-coordination, initially observed in a dimethylthallium complex [18], is now well documented in more than thirty structures [19] and has been the subject of some experimental and theoretical discussion [20]. Nevertheless, in the present context, the relevance of the $[PbPh_2(OAc)(TSC^n)]$ structures resides not in the unusual character of the coordination mode of the TSC^- ligand, but in the fact that the involvement of the electron pair of N(2) in the bonding to the metal prevents its participation in the nucleophilic attack on the

Table 5
Selected bond distances (Å) and angles (°) for thiosemicarbazonate complexes.

Bond[a]	$[PbPh_2(OAc)(TSC^8)] \cdot 2MeOH$	$[PbPh_2(OAc)(TSC^{10})] \cdot H_2O$	$[PbPh_2(OAc)(TSC^{11})] \cdot 0.75MeOH$
Pb–C1	2.185(5)	2.172(18)	2.188(9)
Pb–C2	2.186(6)	2.164(17)	2.188(10)
Pb–O2	2.419(4)	2.403(10)	2.456(6)
Pb–N2	2.423(4)	2.473(16)	2.445(7)
Pb–S	2.6134(16)	2.620(5)	2.638(2)
Pb–O1	2.617(4)	2.647(12)	2.634(6)
Pb–O3	2.831(4)	2.793(11)	2.772(8)
S–C	1.736(7)	1.736(18)	1.737(9)

C(14)–Pb–C(20)	154.3(2)	C(21)–Pb–C(15)	157.5(7)	C(21)–Pb–C(31)	157.7(4)
N(2)–Pb–S	63.5(3)	N(2)–Pb–S(1)	62.5(4)	N(2)–Pb–S	60.8(2)
O(2)–Pb–S	77.79(10)	N(2)–Pb–O(1)	73.4(5)	O(3)–Pb–S	80.14(18)
N(2)–Pb–O(1)	74.3(3)	O(4)–Pb–S(1)	78.6(3)	O(3)–Pb–O(2)	49.1(2)
O(1)–Pb–O(3	96.09(13)	O(3)–Pb–O(1)	96.3(4)	O(1)–Pb–O(2)	92.8(2)
O(2)–Pb–O(3)	48.54(13)	O(3)–Pb–O(3)	49.5(4)	N(2)–Pb–O(1)	77.4(3)

[a]

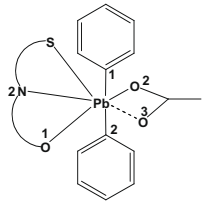

$C(O)R_3$ group and the subsequent ring formation (see Section 1, the (II) → [III] evolution).

It is interesting to compare these structures with that of $[Zn(^TSC^9)_2]$ [7b]. In the zinc complex the ligand behaves in the more usual way and exhibits N(3),S-coordination; there is also an N(4)–H···N(2) hydrogen bond that involves the N(2) electron pair and the O(1) atom is located away from the metal centre, making any Zn–O(1) interaction impossible. Thus, it seems that, as suggested previously [21], small differences in weak interactions or in the steric requirements of the packing may determine which of the N(2),S- or N(3),S-coordination modes is adopted.

In the three complexes an intermolecular $[N(4)–H(4)\cdots O_{acetate}]$ hydrogen bond (Table 4) associates the molecules into chains; other bonds involving the solvent molecules (MeOH or H_2O) link these chains to form a layered network (Figs. 2S–7S).

With respect to the complexes containing the cyclized ligand, the arrangement of the dimers of $[PbPh_2(OAc)(L^5)]\cdot MeOH$ is shown in Fig. 5 and the asymmetric unit of $[PbPh_2Cl(L^2)]$ is represented in Fig. 6. Both figures include a numbering scheme in keeping with that used above for the uncyclized ligands. Selected bond lengths and angles are listed in Table 6.

In the former complex, the metallic atom is coordinated to the S and N(3) atoms of the monodeprotonated pyrazolone, to one oxygen atom of the acetate group [Pb–O(2) = 2.343(3) Å] and, more weakly, to the $O(3)^i$ (i = x, $-y+1$, $-z$) atom belonging to an acetate from a neighbouring molecule [$Pb–O(3)^i$ = 2.721(4) Å]. Thus, the acetate is bis-monodentate and bridges between the two diphenyllead(IV) units to give the dimeric arrangement displayed in Fig. 5. The intramolecular Pb···O(3) distance in the monomer (3.08 Å) is too long to represent a significant interaction.

The geometry around the metal is distorted octahedral and the pyrazolonate shows, in comparison to the free ligand [22], the expected structural evolution [2]. The intermolecular hydrogen bonds $N(1)–H(1B)\cdots O(1S)^{ii}$ and O(1S)–H(1S)···O(1), involving the solvent molecule and the amino and carbonyl groups of the L^- ligand (see Table 4), link the dimers to form a chain (Figs. 8S and 9S).

In $[PbPh_2Cl(L^2)]$ (Fig. 6) the monodeprotonated pyrazolone is N(3),S-coordinated to one diphenyllead(IV) cation and O(1)-bound to another, bridging between the metal centres and connecting the molecules to form a chain (Figs. 10S and 11S). The $Pb–O(1)^i$ distance [2.581(7) Å] is shorter than that in $[Pb(L^7)_2]$ [2.727(3) Å] [2], in which two intermolecular $Pb\cdots O(1)^x$ interactions also exist but the repulsive effect of a stereochemically active lone electron pair on Pb(II) also hinders the intermolecular approach. It is remarkable that the adopted structure contains only bridging pyrazolonates but not bridging chlorides, thus confirming the significant affinity of the diphenyllead(IV) cation with the oxygen donor centres.

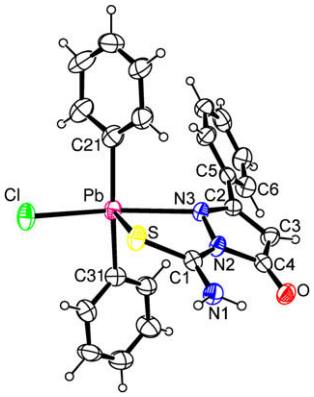

Fig. 6. Asymmetric unit of $[PbPh_2Cl(L^2)]$.

Table 6
Selected bond distances (Å) and angles (°) for pyrazolonate complexes.

Bond[a]	$[PbPh_2Cl(L^2)]$[b]		$[PbPh_2(OAc)(L^5)]\cdot MeOH$[c]
Pb–C(5)	2.173(13)		2.178(4)
Pb–C(6)	2.171(12)		2.166(4)
Pb–N(3)	2.562(8)		2.516(3)
Pb–S	2.686(3)		2.7031(10)
Pb–O(2)	–		2.343(3)
$Pb–O(3)^i$	–		2.721(4)
$Pb–O^i$	2.581(7)		–
Pb–Cl	2.625(3)		–
C–S	1.704(11)		1.710(4)
C(31)–Pb–C(21)	164.6(4)	C(15)–Pb–C(9)	162.67(16)
$N(3)–Pb–O^i$	104.5(2)	O(2)–Pb–S	72.72(8)
N(3)–Pb–S	70.35(18)	$O(2)–Pb–O(3)^i$	106.48(12)
O^i–Pb–Cl	101.07(18)	N(3)–Pb–S	70.33(8)
Cl–Pb–S	84.15(9)	$N(3)–Pb–O(3)^i$	110.36(12)

[a]
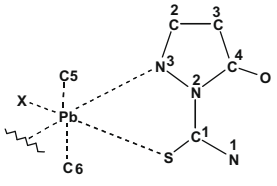

[b] i: $-x+3/2$, $y-1/2$, $-z+1/2$.
[c] i: $-x$, $-y+1$, $-z$.

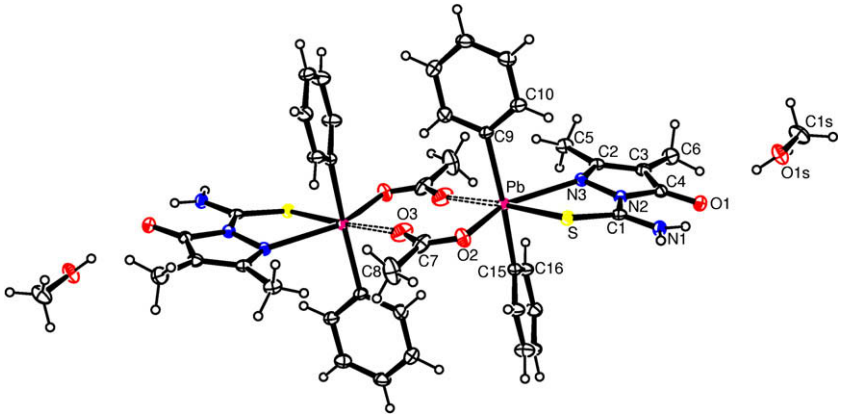

Fig. 5. Dimers of $[PbPh_2(OAc)(L^5)]\cdot MeOH$.

Once again the metal has octahedral coordination, with the main distortion caused by the C(21)–Pb–C(31) angle, which is 164.6(4)° rather than 180°, and the short N(3),S-bite of the ligand [N(3)–Pb–S = 70.35(18)°], which clearly differs from the ideal 90°.

In the crystal lattice, the chains interact via the N(1)–H(1B)···Cl^{ii} intermolecular hydrogen bond (Table 4) to give a layered arrangement (Figs. 10S and 11S).

3.3. IR spectroscopy

The most significant IR bands of the complexes are listed in Section 2 and were assigned according to a previous study [2].

In the spectra of the thiosemicarbazonates [$PbPh_2(OAc)(TSC^n)$] and [$PbPh_2(TSC^n)_2$], the ν(C=N) vibration remains close to its position in the spectra of the free ligands, which is consistent with N(3) not participating in the coordination to the metal. However, the ν(C=S) vibration is shifted to lower wavenumbers, as one would expect if there is a thione to thiol evolution due to the formation of a Pb–S bond. Thus, in this type of complex the TSC^- ligand is probably N(2),S-bound. The acetate ν_{as}(COO) and ν_s(COO) vibration modes lie at positions in keeping with a general anisobidentate OAc^- coordination [23].

In the pyrazolonate complexes the position of the band associated with the ν(C=S) changes upon metallation to lower wavenumber with respect to the free HL^n, suggesting the coordination of the sulfur atom to the metal in all of these pyrazolone complexes. The behaviour of the ν(C=N) mode is similar in all derivatives (a shift to higher wavenumber with respect to the free pyrazolone) and this is consistent with the coordination of N(3) as in [$PbPh_2(OAc)(L^5)$] · MeOH and [$PbPh_2Cl(L^2)$]. As indicated previously [7b], coordination of the oxygen atom of the carbonyl group to the metal cannot be confirmed by the modification of the band associated with ν(C=O) because this mode is also sensitive to the metallation of N(3) and to the changes in the hydrogen bonding interactions involving the carbonyl group. Thus, in [$PbPh_2(OAc)(L^5)$] · MeOH this signal is shifted by approximately 30 cm^{-1} to lower wavenumbers with respect to its position in HL^5, although the X-ray study showed (Fig. 5) that the C=O group is not involved in the coordination to the metal. However, in [$PbPh_2Cl(L^2)$], in which an O(1)–Pb bond exists, ν(C=O) was shifted to lower wavenumbers compared to the corresponding absorption in HL^2 and this shift was only marginally larger (*ca.* 40 cm^{-1}).

As far as the acetate ligand in the heteroleptic [$PbPh_2(OAc)(L^n)$] complexes is concerned, the value of $\Delta\nu$ (=[ν_{as}(COO)– ν_s(COO)]) (150–170 cm^{-1}) suggests a coordination behaviour similar to that described for [$PbPh_2(OAc)(L^5)$] [23].

3.4. ^{1}H, ^{13}C and ^{207}Pb NMR spectra

The ^{1}H, ^{13}C and ^{207}Pb NMR data for the complexes in DMSO–d_6 solution are included in Section 2. The corresponding data for the ligands $HTSC^n$ (n = 1–10) and HL^n (n = 1–7) have been published previously [3,7]. In cases where a long acquisition time was necessary to obtain a spectrum, some of the complexes decomposed to give a black precipitate (possibly PbS), benzene (as shown by new signals at 7.35 and 128.3 ppm in the ^{1}H and ^{13}C NMR spectra, respectively) and, in the case of heteroleptic complexes, diphenyllead acetate (according to the observed ^{207}Pb NMR signal at −863 ppm). This phenomenon was not explored further.

In the ^{1}H and ^{13}C NMR spectra of the thiosemicarbazonate complexes the signals belonging to the TSC^- moiety change with respect to those of the free ligand in the expected way: (i) that of the N(2)H group disappears due to deprotonation; (ii) the two bands associated with the –N(1)H_2 group [2] evolve to give a broad signal, in accordance with the free rotation of this group around the N(1)–C(S) bond as a result of the HTSC deprotonation and metallation; (iii) the C(2) signal is displaced to lower field (by between 6 and 16 ppm) upon complexation, probably due to the bonding of N(3) to the lead atom [7b].

In cases where the signals of the organometallic moiety did not overlap with the aromatic proton signals of the ligand, and therefore could be located, they showed chemical shifts that were very similar in all the complexes and also $^3J(^1H–^{207}Pb)$ values close to 112 Hz. In the ^{13}C NMR spectra the $^2J(^{13}C–^{207}Pb)$ coupling constants are between 87 and 88 Hz. These values are lower than those obtained for diphenyllead compounds with CN = 6 and even lower than those with CN = 5 [24,25], which suggests that in these compounds CN = 4. This low CN is also supported by the ^{207}Pb chemical shift (δ = −294 ppm), which is identical in all compounds and is displaced to lower field by almost 200 ppm with respect to the values reported for other diphenyllead complexes with CN 6 or 5 [24,25].

All of these data suggest that the solid state structures of the complexes [$PbPh_2(OAc)(TSC^n)$] (n = 8, 10 and 11), in which the metal exhibits a CN = 7, are modified in DMSO solution to form species in which the diphenyllead is probably only bound to the TSC^- anion via its S and N(3) atoms. If this is the case, it must be concluded that the NMR parameters of the diorganolead moiety are sensitive, as can been expected, to the CN of the metal and to the identity of the donor atoms, but is rather insensitive to the donor strength of these atoms.

In the pyrazolonate complexes, the main changes in the ^{1}H and ^{13}C NMR spectra of the pyrazolone moiety regarding the free HL^n ligands are: (i) the absence of the signal associated with the N(3)H group; (ii) the slight shielding of C(1) and (iii) the significant deshielding of C(2). The former modification is a consequence of the deprotonation of the ligand and the latter two suggest that the S,N(3)–Pb bonding is retained in DMSO solution.

The values of the $^3J(^1H–^{207}Pb)$ constants, in cases where they could be observed, are in the range 204–210 Hz and this is consistent with a CN of 6 or higher [24]. The limited availability of ^{207}Pb chemical shift data precludes any general conclusions, but this parameter in the cases of [$PbPh_2(L^3)_2$] (−738.1) and [$PbPh_2(L^6)_2$] (−706.4) also suggests a CN of 6 or higher [25–27]. However, the chemical shift value in [$PbPh_2(OAc)(L^6)$] (−869.5) indicates that during the acquisition of the spectrum this complex evolved to give diphenyllead acetate. The complex [$PbPh_2(OAc)(L^5)$] shows two signals, one at −575 and another at −871.9, and this underwent a partial or total displacement of the AcO^- ligand in solution to give a new complex with a lower CN and $PbPh_2(OAc)_2$.

Acknowledgements

We thank the Secretariat General for Research and Development of the Xunta de Galicia (Spain) and the Spanish Ministry of Science and Technology for financial support under Projects PGIDIT03PXIC20306PN, CTQ2006-11805-BQU and BQU2002-04524-C02-01.

Appendix A. Supplementary data

CCDC 712077, 712078, 712079, 712080, 712081 and 712082 contains the supplementary crystallographic data for $HTSC^{10}$, [$PbPh_2(OAc)(TSC^8)$]·2MeOH, [$PbPh_2(OAc)(TSC^{10})$]·H_2O, [$PbPh_2(OAc)(TSC^{11})$]·0.75MeOH, [$PbPh_2(OAc)(L^5)$]·MeOH and [$PbPh_2Cl(L^2)$], respectively. These data can be obtained free of charge via http://www.ccdc.cam.ac.uk/conts/retrieving.html, or from the Cambridge Crystallographic Data Centre, 12 Union Road, Cambridge CB2 1EZ, UK; fax: (+44) 1223-336-033; or e-mail: deposit@ccdc.cam.ac.uk. Supplementary data associated with this article can be found, in the online version, at doi:10.1016/j.poly.2009.01.004.

References

[1] K.N. Zelenin, V.V. Alekseyev, Top. Heterocycl. 1 (1996) 141.
[2] J.S. Casas, E.E. Castellano, J. Ellena, M.S. García-Tasende, A. Sánchez, J. Sordo, A. Touceda, S. Vázquez-Rodríguez, Polyhedron 26 (2007) 4228.
[3] J.S. Casas, M.V. Castaño, M.S. García-Tasende, E. Rodríguez-Castellón, A. Sánchez, L.M. Sanjuán, J. Sordo, Dalton Trans. (2004) 2019.
[4] R.D. Hancock, A.E. Martell, J. Chem. Ed. 73 (1996) 654.
[5] J.S. Casas, E.E. Castellano, J. Ellena, M.S. García-Tasende, A. Sánchez, J. Sordo, A. Touceda, Polyhedron 27 (2008) 1.
[6] S. Jayasree, K.K. Aravindakshan, Polyhedron 12 (1993) 1187.
[7] (a) J.S. Casas, M.V. Castaño, E.E. Castellano, M.S. García-Tasende, A. Sánchez, M.L. Sanjuán, J. Sordo, Eur. J. Inorg. Chem. (2000) 83;
(b) J.S. Casas, M.V. Castaño, E.E. Castellano, J. Ellena, M.S. García-Tasende, A. Gato, A. Sánchez, L.M. Sanjuán, J. Sordo, Inorg. Chem. 41 (2002) 1550;
(c) J.S. Casas, M.V. Castaño, M.S. García-Tasende, A. Sánchez, J. Sordo, A. Touceda, Polyhedron 24 (2005) 3057.
[8] S.G. Schäfer, R.L.F. Davies, B. Elsenhans, W. Forth, K. Schümann, in: H. Marquardt, S.G. Schäfer, R.O. McClellan, F. Welsch (Eds.), Toxicology, Academic Press, San Diego, CA, 1999 (Chapter 32).
[9] G.M. Sheldrick, SHELX-97, An Integrated System for Solving and Refining Crystal Structures from Diffraction Data, University of Göttingen, Göttingen, Germany, 1997.
[10] R.H. Blessing, Acta Crystallogr. A51 (1995) 33.
[11] G.M. Sheldrick, SADABS, Program for Empirical Absorption Correction of Area Detector Data, University of Göttingen, Göttingen, Germany, 1997.
[12] L.J. Farrugia, ORTEP III for Windows, J. Appl. Crystallogr. 30 (1997) 565.
[13] A.L. Spek, PLATON 99, A Multipurpose Crystallographic Tool, University of Utrecht, Utrecht, The Netherlands, 1999.
[14] I.J. Bruno, J.C. Cole, P.R. Edgington, M.K. Kessler, C.F. Macrae, P. McCabe, J. Pearson, R. Taylor, MERCURY, New Software for Searching the Cambridge Structural Database and Visualising Crystal Structures, Acta Crystallogr. B58 (2002) 389.
[15] J.S. Casas, M.V. Castaño, M.C. Cifuentes, J.C. García-Monteagudo, A. Sánchez, J. Sordo, A. Touceda, J. Organomet. Chem. 692 (2007) 2234.
[16] K.A. Jensen, in: P. Grandjean, E.C. Grandjean (Eds.), Biological Effects of Organolead Compounds, CRC Press, Boca Raton, Florida, 2000, p. 3.
[17] J.S. Casas, M.S. García-Tasende, J. Sordo, Coord. Chem. Rev. 209 (2000) 197.
[18] J.S. Casas, E.E. Castellano, A. Macías, M.C. Rodríguez-Argüelles, A. Sánchez, J. Sordo, J. Chem. Soc., Dalton Trans. (1993) 353.
[19] F.H. Allen, Acta Crystallogr. B58 (2002) 380.
[20] D. Mishra, S. Naskar, M.G.B. Drew, S.K. Chattopadhyay, Polyhedron 24 (2005) 1861 and references therein.
[21] J.S. Casas, E.E. Castellano, J. Ellena, M.S. García-Tasende, A. Sánchez, J. Sordo, A. Touceda-Varela, Inorg. Chem. Commun. 7 (2004) 1109.
[22] R. Carballo, J.S. Casas, E. García-Martínez, G. Pereiras-Gabián, A. Sánchez, J. Sordo, E.M. Vázquez-López, Acta Crystallogr. E58 (2002) o787.
[23] K. Nakamoto, Infrared and Raman Spectra of Inorganic and Coordination Compounds, 5th Ed., John Wiley and Sons, New York, 1997.
[24] N. Ólafsson, C.N. Flensburg, P. Andersen, J. Chem. Soc., Dalton Trans. (2000) 4360.
[25] D.G. Calatayud, E. López-Torres, A. Mendiola, Inorg. Chem. 46 (2007) 10434.
[26] M. Schürmann, H. Friedo, J. Organomet. Chem. 530 (1997) 121.
[27] D. Weber, S.H. Hausner, A. Eisengräber-Pabst, S. Yun, J.A. Kraese-Bauer, H. Zimmer, Inorg. Chim. Acta 357 (2004) 125.